Vacuum ultraviolet photodissociation and surface morphology change of water ice films dosed with hydrogen chloride

Akihiro Yabushita, Daichi Kanda, Noboru Kawanaka, and Masahiro Kawasaki[a)]
Department of Molecular Engineering, Kyoto University, Kyoto 615-8510, Japan

(Received 6 March 2007; accepted 12 September 2007; published online 19 October 2007)

Time-of-flight (TOF) spectra of photofragment H atoms from the photodissociation of water ice films at 193 nm were measured for amorphous and polycrystalline water ice films with and without dosing of hydrogen chloride at 100–145 K. The TOF spectrum is sensitive to the surface morphology of the water ice film because the origin of the H atom is the photodissociation of dimerlike water molecules attached to the ice film surfaces. Adsorption of HCl on a polycrystalline ice film was found to induce formation of disorder regions on the ice film surface at 100–140 K, while the microstructure of the ice surface stayed of polycrystalline at 145 K with adsorption of HCl. The TOF spectra of photofragment Cl atoms from the 157 nm photodissociation of neutral HCl adsorbed on water ice films at 100–140 K were measured. These results suggest partial dissolution of HCl on the ice film surface at 100–140 K. © *2007 American Institute of Physics*.
[DOI: 10.1063/1.2794342]

I. INTRODUCTION

There has been a widespread interest in characterizing HCl adsorption at the ice surface and probing the morphology change by adsorption of HCl on water ice surfaces because morphology may have a significant effect on the reactivity of ice films.[1] Adsorption, desorption, surface mobility, and bulk diffusion of reagents and reaction products may depend on the ice microstructure because pores facilitate trapping of large quantities of gases in the bulk of amorphous ice films, and a high density of surface defects leads to an increase in the hydrogen bonding abilities of crystalline ice films. However, conventional spectroscopic techniques probe both surface and bulk phases except for a technique using atom collisions. Hence, a new technique is required to investigate effects of adsorption of molecules on the morphology of ice films.

In our previous experiments, we have shown that hydrogen atoms are produced as primary photoproducts when dimerlike water molecules on the outermost layer of a polycrystalline ice film are dissociated at 193 nm based on the fact that the photoabsorption of the branched water cluster is redshifted compared with that of cyclic water clusters.[2]

$$H_2O-(H_2O)_n + h\nu(193\ \text{nm}) \rightarrow H + HO-(H_2O)_n. \quad (1)$$

In the 193 nm photodissociation of a crystalline ice film, the time-of-flight (TOF) spectra of the H atoms consisted solely of a fast component of the Maxwell-Boltzmann energy distribution. However, a slow component became dominant from an amorphous ice film due to the collisional relaxation process of the photofragment H atoms in the micropores on the surface. Thus, if the ice surface morphology is distorted by dosing with HCl, a change in the TOF spectrum of the H atoms is expected. This TOF technique could be a sensitive method to investigate the surface morphology change of water ice films.

There are numerous reports of experimental and theoretical studies on the interactions of ice films with HCl. For example, Kang *et al.* observed the transformation of HCl adsorbed on ice surfaces from a predominantly molecular form to an ionic species during heating from 50 to 140 K.[3] In the present study, using the TOF techniques we have studied morphology change of the outermost layer of ice films by dosing with HCl as a function of temperature. We will compare our results with the previously reported studies on the interaction, and discuss the origins of the H atoms from the vacuum ultraviolet photodissociation of water ice films dosed with HCl.

II. EXPERIMENT

The experimental apparatus and procedures of ice film preparation have been described elsewhere.[4] Photodissociation of water ice films was carried out in a high vacuum chamber, which was equipped with two turbo molecular pumps in tandem. Ice films were prepared on polycrystalline Au substrates with (111) domains.[5] Two types of ice films were used in this experiment: amorphous solid water (ASW) and polycrystalline ice (PCI) films. ASW films were prepared with background (backfill) deposition at 100 K for 60 min. The exposure of water vapor was typically 1800 L ($1\ \text{L} = 1 \times 10^{-6}$ Torr s), which resulted in the formation of 600 ML of H_2O on the Au substrate.[6] PCI films were prepared by background deposition of water vapor at 130 K for 60 min, and then maintained at this temperature for a further 30 min for annealing purposes.

The gas mixture of HCl with N_2 diluent (4%) was introduced into the vacuum chamber via direct or background deposition with a pulsed molecular beam. A typical stagnation pressure of a pulsed gas valve for the mixture gas was 40 Torr. The chamber pressure was 5×10^{-8} without sample

[a)]Author to whom correspondence should be addressed. FAX: +81-75-383-2573. Electronic mail: kawasaki@photon.mbox.media.kyoto-u.ac.jp

molecule injection. This adsorption resulted in the formation of 1 ML of HCl on the ice film since multilayer formation of HCl does not occur.[7] When HCl was dosed up to a few tens of langmuirs, the signal intensity increased with dose rate up to 2 L, and approached an asymptotic value for >2 L. The 193 nm laser light (Lambda Physik, COMPex, ArF) was directed onto the ice film using a series of aluminum mirrors and a prism resulting in an incident fluence of 1 mJ cm^{-2} $pulse^{-1}$. The 157 nm photolysis beam (Lambda Physik, OPTexPro, F_2) was introduced directly on the ice surface (fluence < 1 mJ cm^{-2} $pulse^{-1}$). Hydrogen atom photofragments were subsequently ionized at a distance of 3 mm from the substrate surface by [2+1] resonance enhanced multiphoton ionization (REMPI) on the $H(2s \leftarrow 1s)$ transition with a lens (f=0.10 m) and collected with a small TOF mass spectrometer aligned perpendicular to the ice surface. The requisite radiation at wavelengths ~243.135 nm was produced by a neodymium-doped yttrium aluminum garnet pumped dye laser (Lambda Physik, SCANmate, 0.2 mJ $pulse^{-1}$ at UV) using Coumarin 480 dye, followed by subsequent frequency doubling with a BaB_2O_4 crystal. Each spectrum is the sum of several spectra measured at different Doppler shifted wavelengths around that required for the REMPI detection. This laser was also used to ionize the photofragment by (2+1) REMPI at 235.336 nm for $Cl(^2D_{3/2} \leftarrow {}^2P_{3/2})$ and 235.205 nm for $Cl^*(^2P_{1/2} \leftarrow {}^2P_{1/2})$. For each spin-orbit state, the REMPI intensity I depends both on the quantum state population N and the ionization efficiency S. Thus, $I(Cl^*)/I(Cl)=[N(Cl^*)/N(Cl)][S(Cl^*)/S(Cl)]$. The scaling factor, $S(Cl^*)/S(Cl)$, was reported to be 1.06±0.17 by Regan *et al.*[8]

TOF spectra of H atoms were taken as a function of time delay t between photolysis and probe pulses, which correspond to the flight time between the substrate and the detection region. The TOF spectrum was fitted with $S(t,a_i,T_i)$, consisting of three flux-weighted Maxwell-Boltzmann (MB) distributions defined by the translational temperature T_i and a coefficient a_i:

$$S(t,a_i,T_i) = a_1 S_{\mathrm{MB}}(t,T_1) + a_2 S_{\mathrm{MB}}(t,T_2) + (1-a_1-a_2) S_{\mathrm{MB}}(t,T_3), \quad (2)$$

$$S_{\mathrm{MB}}(t,r) = r^3 t^{-4} \exp[-mr^2/(2k_{\mathrm{B}}T_{\mathrm{trans}}t^2)], \quad (3)$$

$$P_{\mathrm{MB}}(E_t) = (k_{\mathrm{B}}T_{\mathrm{trans}})^{-2} E_t \exp[-E_t/(k_{\mathrm{B}}T_{\mathrm{trans}})], \quad (4)$$

where r is a flight length for the photofragment. The MB distribution, $P_{\mathrm{MB}}(E_t)$, as a function of translational energy E_t is characterized by the average translational energy, $\langle E_t \rangle = 2k_{\mathrm{B}}T_{\mathrm{trans}}$, where k_{B} is the Boltzmann constant and T_{trans} is the translational temperature. Conversion from the energy distribution to the TOF distribution was performed using the Jacobian listed by Zimmermann and Ho.[9]

In order to simulate the obtained TOF spectra of Cl atoms, we used a composite of normalized TOF functions, $S_G(t)$ and $S_{\mathrm{MB}}(t)$. These functions correspond to a Gaussian translational energy distribution, $P_G(E_t)$, and a flux-weighted MB energy distribution, $P_{\mathrm{MB}}(E_t)$, respectively. $P_G(E_t)$ is characterized by the average energy, $\langle E_t \rangle$, and the energy width w.

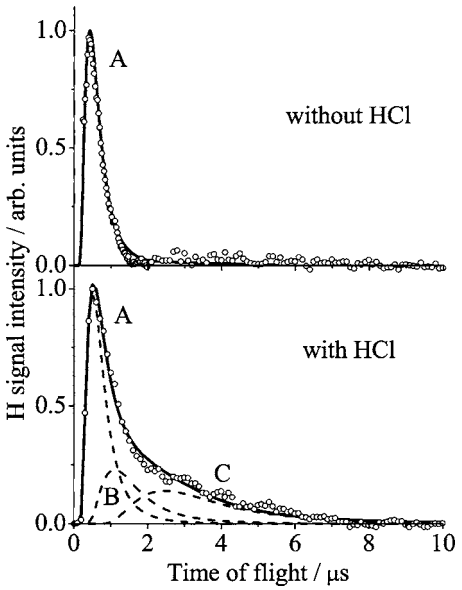

FIG. 1. Time-of-flight spectra of H atoms from the 193 nm photodissociation of polycrystalline ice films with and without HCl (1 ML) at 100 K (open circles). The solid curves are fits to the data derived assuming a Maxwell-Boltzmann distribution with T_{trans}=2400 K for component A (upper panel), and the sum of three distributions with T_{trans}=2400 K for A, 500 K for B, and 110 K for C (lower panel). Contributions of the Maxwell-Boltzmann components are listed in Table I.

$$S(b,t) = bS_G(t) + (1-b)S_{\mathrm{MB}}(t), \quad (5)$$

$$P_G(E_t) = [(2\pi)^{1/2}w]^{-1} \exp[-2(E_t - \langle E_t \rangle)^2/w^2], \quad (6)$$

where b is a coefficient. The details of simulation of the TOF spectra were described in our previous paper.[4]

III. RESULTS

A. Time-of-flight spectra of hydrogen atoms from the photodissociation of water ice films with and without dosing of HCl at 193 and 157 nm

Figure 1 shows the TOF spectra of H atoms from the 193 nm photodissociation of PCI films with and without dosing of HCl (1 ML) at 100 K. The TOF spectrum for the ice film without HCl is well described by the fast component A with T_{trans}=2400±100 K ($\langle E_t \rangle$=0.31±0.01 eV). Upon dosing with HCl, additional signals appeared in the TOF spectrum, and the intensity of component A stayed almost the same. The TOF spectrum is reproduced by summing three different MB distributions: the fast component A with T_{trans}=2400±100 K contributing (47±7)% and the surface-accommodated slow component C with T_{trans}=110±10 K (0.01 eV) (32±10)%. The residual TOF signal is approximated by a single MB distribution, the middle component B with T_{trans}=500±50 K (0.06 eV) (21±3)%. The signal of the B and C components appeared even at a dose rate of 0.06 L. Its intensity increased with dose rate up to 2 L, and became an asymptotic value for >2 L.

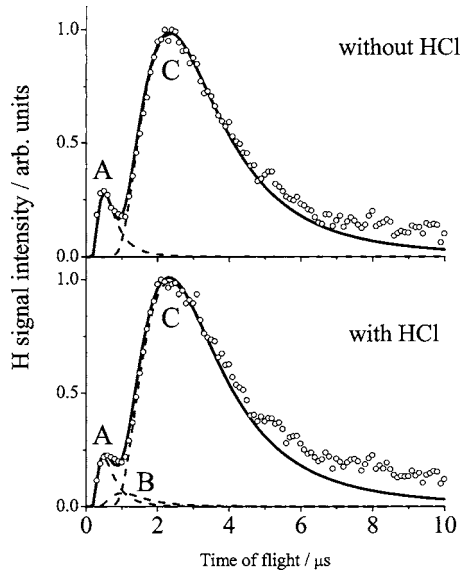

FIG. 2. TOF spectra of H atoms from the 193 nm photodissociation of amorphous solid water films with and without HCl (1 ML) at 100 K. Fits are to three Maxwell-Boltzmann distributions with T_{trans}=2400 K for A, 500 K for B, and 110 K for C. Contributions of components A, B, and C are listed in Table I.

Figure 2 shows the TOF spectra from the 193 nm photodissociation of ASW films at 100 K with and without HCl (1 ML). Both spectra are similar to each other, and consist mainly of component C. There are very small contributions of components A and B.

The upper panel of Fig. 3 shows the TOF spectra from the 157 nm photodissociation of PCI films at 100 K with and without HCl (1 ML). Both spectra are essentially the same. Three MB components, A′, B′, and C, are characterized by T_{trans}=4750±250 K (0.61±0.04 eV) contributing (41±3)%, 625±25 K (0.08 eV) (44±4)%, and 110±10 K (0.01 eV) (15±5)%, respectively. The lower panel of Fig. 3 shows the TOF spectra from the 157 nm photodissociation of ASW films at 100 K with and without HCl (1 ML), which are essentially the same, and represented by summing three MB components, A′[(5±2)%], B′[(12±2)%], and C[(83±4)%]. Table I summarizes the contribution and translational temperature of each component.

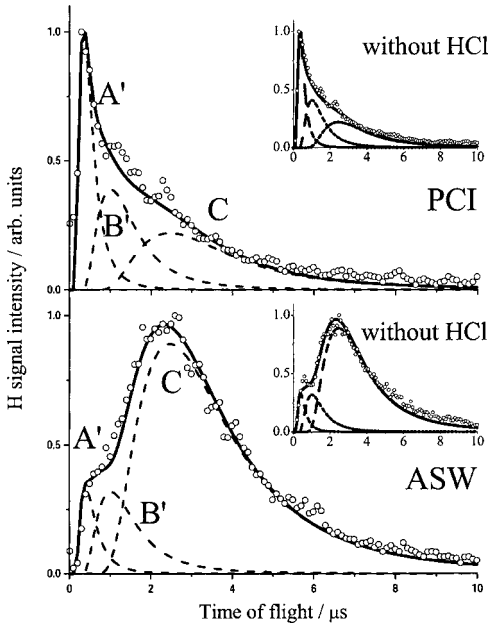

FIG. 3. The upper panel shows TOF spectra of H atoms from the 157 nm photodissociation of polycrystalline ice (PCI) films with HCl (1 ML) at 100 K. The inset shows the spectrum without HCl. Fits are to three Maxwell-Boltzmann distributions with T_{trans}=4750 K for A′, 625 K for B′, and 110 K for C. The lower panel shows TOF spectra of H atoms from the 157 nm photodissociation of amorphous solid water (ASW) films with HCl (1 ML) at 100 K. The inset shows the spectrum without HCl. Fits are to three Maxwell-Boltzmann distributions with T_{trans}=4750 K for A′, 625 K for B′, and 110 K for C. Contributions are listed in Table I.

B. Substrate temperature dependence of the time-of-flight spectra of hydrogen atoms from the 193 nm photodissociation of polycrystalline ice films dosing with HCl

Figure 4 shows the substrate temperature dependence of TOF spectra of the H atoms from the 193 nm photodissociation of PCI films with HCl (1 ML). PCI films were prepared and exposed to HCl at 100 K, and then maintained at four different substrate temperatures, T_s=100, 120, 140, and 145 K for a further 30 min. And then, the substrate temperature was reduced to 100 K during the TOF measurements. In the obtained TOF spectra, the contributions of components B and C gradually decreased with T_s up to 140 K, and finally disappeared at 145 K. The surface composition of the thus-prepared film is not changed by cooling it from 140 to 100 K.[10]

C. Time-of-flight spectra of chlorine atoms from the photodissociation of molecular HCl adsorbed on water ice films at 157 nm

Figure 5 shows the TOF spectra of $Cl(^2P_{3/2})$ and $Cl^*(^2P_{1/2})$ atoms from the 157 nm photodissociation of ASW films dosed with HCl (1 ML) at 100 K. The TOF spectra are reproduced by a combination of the Gaussian and MB distributions. The Gaussian distribution of $Cl(^2P_{3/2})$ is characterized by $\langle E_t\rangle_{Cl}$=1.4±0.1 eV, w_{Cl}=0.9±0.1 eV contributing (2±1)%. The MB distribution is characterized by $T_{trans}(Cl)$ =1700±100 K (0.22±0.01 eV) (98±1)%. For Cl^*, $\langle E_t\rangle_{Cl^*}$ is 1.4±0.1 eV, w_{Cl^*}=0.9±0.1 eV contributing (3±1)%. The MB distribution is characterized by $T_{trans}(Cl^*)$ =2800±200 K (0.36±0.03 eV). The branching ratio, $[Cl^*]/[Cl]$, was 0.08±0.03.

Figure 6 shows the TOF spectra from the PCI film dosed with HCl (1 ML) at 100 K. The Gaussian and MB distributions are characterized by the parameters listed in Table II. $[Cl^*]/[Cl]$ was 0.04±0.02. These branching ratios did not change when the dose rate was increased from 2 L (corresponding to 1 ML) up to a few tens of langmuirs since multilayer formation of HCl does not occur.[7]

We have also examined the substrate temperature dependence of TOF spectra, which are shown in Fig. 6. PCI films were exposed with HCl (1 ML) at 100 and 140 K. For the 140 K the substrate temperature was kept for a further 30 min. Then, the substrate temperature was reduced to 100 K during TOF measurements. The TOF spectra are re-

TABLE I. Contributions and translational temperatures of the Maxwell-Boltzmann (MB) components for the time-of-flight spectra of H atoms from ASW and PCI films at 193 and 157 nm. Substrate temperature was kept at 100 K. ASW=amorphous solid water. PCI=polycrystalline ice. Coverage of HCl was 1 ML.

Dissociation wavelength (nm)	Type of ice film	Contribution of MB components (%)		
		A (2400±100 K)	B (500±50 K)	C (110±10 K)
193	PCI without HCl	100	—	—
	PCI with HCl	47±7	21±3	32±10
	ASW without HCl	6±3	—	94±3
	ASW with HCl	4±2	2±2	94±4
Dissociation wavelength (nm)	Type of ice film	Contribution of MB components (%)		
		A (4750±250 K)	B (625±25 K)	C (110±10 K)
157	PCI with and without HCl	41±3	44±4	15±5
	ASW with and without HCl	5±2	12±2	83±4

produced with the parameters listed in Table II. The TOF spectrum on the PCI film exposed with HCl at 140 K is essentially the same as that at 100 K.

We investigated the formation of Cl and Cl^* atoms from the 193 nm photodissociation of the ice films dosed with HCl, but could not detect the REMPI signals.

IV. DISCUSSION

A. Surface morphology changes probed by time-of-flight measurements of hydrogen atoms

1. Origin of hydrogen atoms from the photodissociation of polycrystalline ice films

In our previous experiments at 193 nm (6.4 eV), we have shown that the fast TOF component A from a neat PCI film comes from one-photon dissociation of the dimerlike water molecules on the topmost H_2O layer of the ice film via reaction (1), which have photoabsorption near 200 nm due to the branched form of the water cluster.[2,11] Similarly, Kimmel and Orlando reported threshold energies of 6.5–7.0 eV for desorption of D atoms following electron-beam irradiation on thin films of amorphous D_2O ice.[12] Hence, for the 193 nm photodissociation of the neat PCI film the TOF spectrum of the upper panel of Fig. 1 can be fitted solely by the fast component A. When an ASW film was photoirradiated at 193 nm, however, the TOF spectrum consists mostly of the surface-accommodated slow component C, as shown in the upper panel of Fig. 2. Since the adsorption of HCl induces disordering of the PCI film surface, the slow and middle components C and B appeared in the TOF spectrum, as shown in the lower panel of Fig. 1. Thus, the present TOF spectroscopy is specifically sensitive to disordering of the top surface. If the percentage of disordered surface area is proportional to that of the B and C components in TOF spec-

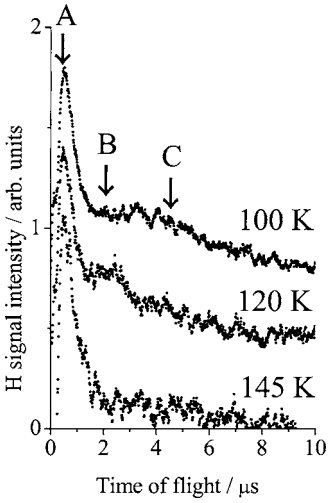

FIG. 4. Substrate temperature dependence of the TOF spectra of H atoms from the 193 nm photodissociation of polycrystalline ice films with HCl (1 ML). After the polycrystalline ice films were exposed to HCl at the indicated temperatures, TOF measurements were performed at 100 K. A, B, and C stand for the Maxwell-Boltzmann translational components listed in Table I.

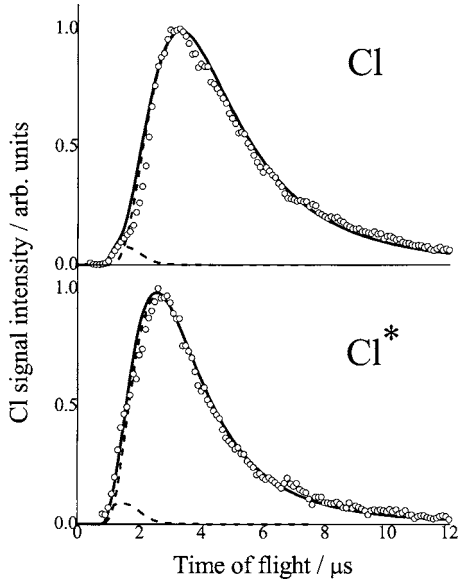

FIG. 5. TOF spectra of $Cl(^2P_{3/2})$ and $Cl^*(^2P_{1/2})$ atoms from the 157 nm photodissociation of amorphous solid water films with HCl (1 ML) at 100 K. The solid curves are fits to the data derived assuming the sum of a Gaussian distribution with $\langle E_t \rangle = 1.40$ eV and a Maxwell-Boltzmann distribution with $T_{trans} = 1700$ K (upper panel), and a Gaussian distribution with $\langle E_t \rangle = 1.40$ eV and a Maxwell-Boltzmann distribution with $T_{trans} = 2800$ K (lower panel). Contributions and translational energies (temperatures) are listed in Table II.

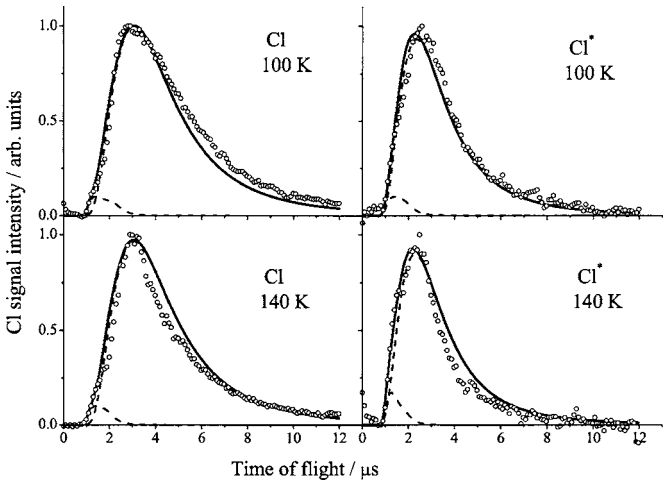

FIG. 6. TOF spectra of Cl and Cl^* from the 157 nm photodissociation of polycrystalline ice films with HCl (1 ML) at 100 and 140 K. The solid curves are the sum of a Gaussian distribution and a Maxwell-Boltzmann distribution. Contributions and translational energies (temperatures) are listed in Table II.

tra, it is estimated to be (53±13)% at the ice temperature of 100 K upon HCl (1 ML) adsorption on a PCI film.

The photoabsorption spectrum of HCl adsorbed on a water ice film was calculated by Woittequand *et al.* using the Fourier transform of the autocorrelation function of a dissociative wave packet.[13] The calculated absorption spectrum of molecular HCl on a PCI film at 0 K is blueshifted by 0.36 eV with respect to the gas phase spectrum because of the surface stabilization in the ground state of molecular HCl attached to the ice surface. Hence, the H atoms from the photodissociation do not come from the 193 nm photodissociation of HCl adsorbed on the PCI surface. This blueshift was confirmed by the experimental results that Cl atoms were not detected in the 193 nm irradiation of the ice films dosed with HCl, but observed at 157 nm.

About the dissociation threshold wavelength, Kimmel and Orlando measured D atoms from the electron-stimulated dissociation (ESD) of amorphous D_2O ice adsorbed on Pt(111) at ~90 K.[12] They reported that a low energy threshold for D atom production is 6.5–7.0 eV. There exists the dissociative electronic state near 200 nm. Their TOF spectra for D atoms consist of two components; one is ejected directly from the surface without interacting to surrounding molecules, and the other is accommodated to the surface temperature prior to desorption. These results are in good agreement with the present TOF results. It is likely that the same electronic excitation and the dynamics occur in the photo- and electron bombardment dissociation.

The TOF spectrum at 157 nm (7.9 eV), the upper inset of Fig. 3, is characterized by summing the three MB distributions because of the bulk ice photodissociation, that is, the fast H atoms generated from the outmost surface correspond to component A′, the H atoms from the bulk phase correspond to component B′, and the translationally relaxed H atoms that are accommodated to the surface temperature correspond to component C.[2] Although molecular HCl has relatively strong photoabsorption at 157 nm, the present TOF spectra with and without HCl in Fig. 3 are very similar to each other, because the population of molecular HCl on the ice surface at 100 K would be small with respect to water molecules in the bulk phase.

2. Origin of hydrogen atoms from the photodissociation of amorphous solid water film

The origin of the H atoms recorded at 193 nm from ASW is attributed to the photodissociation of surface species on ice films, while at 157 nm the H atoms come from the photodissociation of surface and bulk of ice films.[2] Although the origins are different, the TOF spectra at 193 and 157 nm are both dominated by the slow component C, indicating that the photofragment H atoms are accommodated to the substrate temperature by collisions in the micropores of the ASW film surfaces.

B. Surface morphology change of water ice films on adsorption of hydrogen chloride

In the TOF spectra of H atoms from the 193 nm photodissociation of the PCI film with HCl at 100, 120, and 140 K, the signal intensity of component A was almost the same while slow components B and C appeared. The substrate temperature dependence of Fig. 4 shows that the components B and C gradually decreased from 100 to 120 K. At 140 K these components were still present, and then disappeared at 145 K. Dosing with HCl on the ice surface induced

TABLE II. Contribution and translational energies (temperatures) of the Gaussian and the Maxwell-Boltzmann (MB) components for the time-of-flight spectra of $Cl(^2P_{3/2})$ and $Cl^*(^2P_{1/2})$ atoms from the photodissociation of HCl on ASW and PCI films at 157 nm. During the time-of-flight measurements the substrate temperature was kept at 100 K. ASW=amorphous solid water. PCI=polycrystalline ice. Coverage of HCl was 1 ML.

			Gaussian component		MB component	
Chlorine atoms	Adsorption temperatures	Ice film with HCl	Translational energy (eV)	Contribution (%)	Translational temperature (K)	Contribution (%)
Cl	100	ASW	1.4±0.1	2±1	1700±100	98±1
Cl^*		ASW	1.4±0.1	3±1	2800±200	97±1
Cl		PCI	1.4±0.1	3±1	2000±200	97±1
Cl^*		PCI	1.4±0.1	4±1	3600±200	96±1
Cl	140	PCI	1.4±0.1	3±1	2000±200	97±1
Cl^*		PCI	1.4±0.1	7±2	3600±200	93±2

surface disordering below 140 K as discussed above. Adsorption states of HCl on water ice films were investigated by using the reactive ion scattering technique with Cs^+ as a function of ice temperature.[3,7,14] This reactive ion scattering study suggests that for temperatures below 80 K molecular adsorption dominates, while the amount of ionic species increases until an ice temperature of 140 K is reached.[3] This result shows that the ionic dissolution of molecular HCl on ice surfaces is completed around 140 K. Therefore, components B and C disappeared in the present TOF spectrum of H atoms at 145 K.

The TOF spectrum from the ASW film with HCl was not different from that without HCl, because the surface morphology of the ASW film was effectively not changed by dosing with HCl (Fig. 2).

C. Chlorine atoms from photodissociation of molecular HCl adsorbed on water ice films

Since HCl are not completely ionized and molecular HCl remain on the ice surface even at 140 K, Cl or Cl^* atoms were detected from the 157 nm photodissociation of HCl adsorbed on the PCI films (Figs. 5 and 6). Sadtchenko *et al.*[15] reported in their temperature programmed desorption (TPD) experiments that there are three types of adsorption states at 95 K, α-, β-, and σ-HCl. α-HCl was attributed either to molecular HCl adsorbed on the surface of HCl hexahydrate[16] or to a thin HCl-monolayer adlayer formed on the saturated hexahydrate film.[17] β-HCl mainly exists on an ASW film. σ-HCl is characteristic of the PCI surface and is essentially absent at the ASW surface. Table II shows that the translational temperatures of the MB components of chlorine atoms from the photodissociation of molecular HCl on the PCI film are higher than those from the ASW films. The translational temperature difference between the PCI and ASW films might be due to the different populations of three adsorption states, σ-HCl for PCI and β-HCl for ASW.

The branching ratios of Cl^*/Cl from the gas phase photodissociation at 157 nm were experimentally and theoretically obtained to be 0.81 ± 0.09 and ~ 0.67, respectively.[18,19] The present ratios of $Cl^*/Cl(=0.04-0.08)$ from the ice film surface are low because (a) the potential surface distortion changes the transmission probabilities in the potential intersection regions, and (b) the slow velocity of the photofragment results in adiabatic behavior of the dissociation potentials.

D. Molecular states of HCl on water ice films

Depending on the surface temperature, HCl on ice form mono-, tri-, and hexahydrate, or is ionized.[20] As shown in Fig. 7, there are numerous reports of studies on the interactions of HCl with ice films with various experimental methods: temperature-programed desorption mass spectrometry (TPDMS),[15] infrared spectroscopy,[17,21,22] secondary ion mass spectroscopy,[10,23,24] laser thermal desorption,[25] reactive ion scattering (RIS),[3,7,14] near-edge x-ray absorption fine structures (NEXAFSs),[26] electron-stimulated desorption,[27] and molecular beam scattering techniques.[28,29]

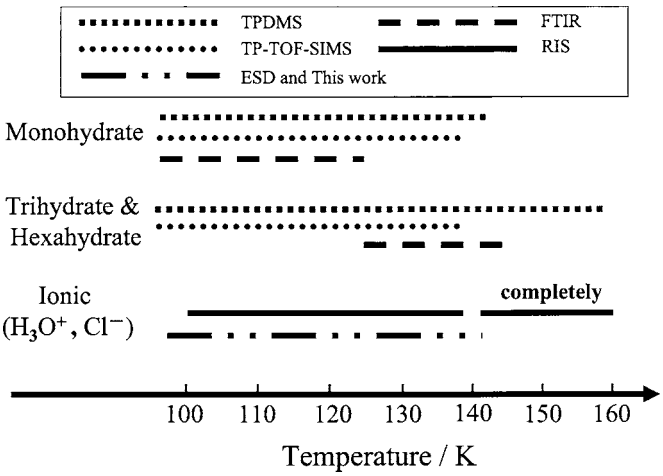

FIG. 7. Molecular adsorption states of HCl of water ice films from references. Temperature-programed desorption mass spectrometry (TPDMS), Ref. 15; temperature-programed time-of-flight secondary-ion mass spectrometry (TP-TPF-SIMS), Ref. 10; electron-stimulated desorption (ESD), Ref. 27; Fourier transform infrared spectroscopy (FTIR), Ref. 21; and reactive ion scattering (RIS), Refs. 7 and 14.

The RIS study suggests that for temperatures below 80 K molecular adsorption dominates, while the amount of ionic species increases until an ice temperature of 140 K is reached.[3] These results are corroborated by the H–Cl bond signal in photostimulated desorption-NEXAFS spectra. At 150 K, this bond is only visible for pure HCl, but not for HCl adsorbed on ice films, which directly demonstrates the dissociation of HCl. Foster *et al.* investigated the interaction of HCl with ice surfaces as a function of ice temperature, using laser-induced thermal desorption techniques.[25] In agreement with the $HCl \cdot H_2O$ phase diagram, a stable $HCl \cdot 3H_2O$ trihydrate consistently formed between 140 and 148 K. Monte Carlo simulations by Devlin *et al.* suggested that a minimum of three hydrogen bonds is needed for HCl ionization.[22] These results show that the ionic dissociation of HCl on ice surfaces is completed between 140 and 150 K, as shown in Fig. 7. Therefore, in the present experiment, components B and C disappeared in the TOF spectrum of H atoms at 145 K (Fig. 4).

V. CONCLUSION

The time-of-flight spectrum of hydrogen atoms from the 193 nm photodissociation of surface water molecules on polycrystalline ice films at 100 K after dosing with HCl (1 ML) is characterized by a combination of three different (fast, medium, and slow) Maxwell-Boltzmann energy distributions, while the spectrum measured without dosing of HCl is fitted solely by the fast component. The appearance of the slow components is attributed to partial disordering of the ice film surface by dosing with HCl. When the ice film temperature was raised to 145 K the medium and slow components did not appear even after dosing with HCl because the surface morphology was kept of polycrystalline structure. The fact that detection of chlorine atoms in the $^2P_{3/2}$ and $^2P_{1/2}$ levels was successful from the 157 nm photodissociation of

molecular HCl on the ice films dosed by HCl at 100–140 K suggests that molecular HCl remain partially on the surface up for 100–140 K.

[1] V. F. McNeill, T. Loerting, F. M. Geiger, B. L. Trout, and M. J. Molina, Proc. Natl. Acad. Sci. U.S.A. **103**, 9422 (2006).
[2] A. Yabushita, D. Kanda, N. Kawanaka, M. Kawasaki, and M. N. R. Ashfold, J. Chem. Phys. **125**, 133406 (2006).
[3] H. Kang, T.-H. Shin, S.-C. Park, I. K. Kim, and S.-J. Han, J. Am. Chem. Soc. **122**, 9842 (2000).
[4] A. Yabushita, Y. Inoue, T. Senga, M. Kawasaki, and S. Sato, J. Phys. Chem. B **106**, 3151 (2002).
[5] M. Kawasaki, Appl. Surf. Sci. **135**, 1159 (1998).
[6] S. Sato, D. Yamaguchi, K. Nakagawa, Y. Inoue, A. Yabushita, and M. Kawasaki, Langmuir **16**, 9533 (2000).
[7] S.-C. Park and H. Kang, J. Phys. Chem. B **109**, 5124 (2005).
[8] P. M. Regan, S. R. Langford, D. Ascenzi, P. A. Cook, A. J. Orr-Ewing, and M. N. R. Ashfold, Phys. Chem. Chem. Phys. **1**, 3247 (1999).
[9] F. M. Zimmermann and W. Ho, Surf. Sci. Rep. **22**, 127 (1995).
[10] M. Kondo, H. Kawanowa, Y. Gotoh, and R. Souda, Surf. Sci. **594**, 141 (2005).
[11] A. Yabushita, Y. Hashikawa, A. Ikeda, M. Kawasaki, and H. Tachikawa, J. Chem. Phys. **120**, 5463 (2004).
[12] G. A. Kimmel and T. M. Orlando, Phys. Rev. Lett. **75**, 2606 (1995).
[13] S. Woittequand, C. Toubin, B. Pouilly, M. Monnerville, S. Briquez, and H.-D. Meyer, Chem. Phys. Lett. **406**, 202 (2005).
[14] H. Kang, Acc. Chem. Res. **38**, 893 (2005).
[15] V. Sadtchenko, C. F. Giese, and W. R. Gentry, J. Phys. Chem. B **104**, 9421 (2000).
[16] J. D. Graham and J. T. Roberts, J. Phys. Chem. **89**, 5974 (1994).
[17] S. F. Banham, J. R. Sodeau, A. B. Horn, M. R. S. McCoustra, and M. A. Chesters, J. Vac. Sci. Technol. A **14**, 1620 (1996).
[18] K. Tonokura, Y. Matsumi, M. Kawasaki, S. Tasaki, and R. Bersohn, J. Chem. Phys. **97**, 8210 (1992).
[19] P. M. Regan, D. Ascenzi, A. Brown, G. G. Balint-Kurti, and A. J. Orr-Ewing, J. Chem. Phys. **112**, 10259 (2000).
[20] T. Huthwelker, M. Ammann, and T. Peter, Chem. Rev. (Washington, D.C.) **106**, 1375 (2006).
[21] S. Haq, J. Harnett, and A. Hodgson, J. Phys. Chem. B **106**, 3950 (2002).
[22] J. P. Devlin, N. Uras, J. Sadlej, and V. Buch, Nature (London) **487**, 269 (2002).
[23] H. A. Donsig and J. C. Vickerman, J. Chem. Soc., Faraday Trans. **93**, 2755 (1997).
[24] M. Kondo, H. Kawanowa, Y. Gotoh, and R. Souda, J. Chem. Phys. **121**, 8586 (2004).
[25] K. L. Foster, M. A. Tolbert, and S. M. George, J. Phys. Chem. A **101**, 4979 (1997).
[26] P. Parent and C. Laffon, J. Phys. Chem. B **109**, 1547 (2005).
[27] J. Herring, A. Aleksandrov, and T. M. Orlando, Phys. Rev. Lett. **92**, 187602 (2004).
[28] M. J. Isakson and G. O. Sitz, J. Phys. Chem. A **103**, 2044 (1999).
[29] J. Harnett, S. Haq, and A. Hodgson, Surf. Sci. **532**, 478 (2003).